Toward global mapping of river discharge using satellite images and at-many-stations hydraulic geometry

Colin J. Gleason[1] and Laurence C. Smith

Department of Geography, University of California, Los Angeles, CA 90095-1524

Edited by James S. Famiglietti, University of California, Irvine, CA, and accepted by the Editorial Board February 18, 2014 (received for review September 17, 2013)

Rivers provide critical water supply for many human societies and ecosystems, yet global knowledge of their flow rates is poor. We show that useful estimates of absolute river discharge (in cubic meters per second) may be derived solely from satellite images, with no ground-based or a priori information whatsoever. The approach works owing to discovery of a characteristic scaling law uniquely fundamental to natural rivers, here termed a river's at-many-stations hydraulic geometry. A first demonstration using Landsat Thematic Mapper images over three rivers in the United States, Canada, and China yields absolute discharges agreeing to within 20–30% of traditional in situ gauging station measurements and good tracking of flow changes over time. Within such accuracies, the door appears open for quantifying river resources globally with repeat imaging, both retroactively and henceforth into the future, with strong implications for water resource management, food security, ecosystem studies, flood forecasting, and geopolitics.

remote sensing | fluvial geomorphology | river hydrology | AMHG | river runoff

Some 80% of the world's population and 65% of its river ecosystems are threatened by insecure water supply, yet global knowledge of the river discharges upon which these depend is surprisingly poor (1, 2). For much of the world, river gauge measurements are rare, nonexistent, or proprietary. Even well-monitored countries have sparsely distributed networks, thus limiting current understanding of water losses along river courses, habitat changes, and flood risk (3, 4). Satellites, in contrast, provide spatially dense coverage globally, attracting calls for a global river discharge mapping capacity from space (5–10). However, previous efforts to estimate river discharge from remotely sensed observations have all required inclusion of some form of ancillary ground-based information, such as gauge measurements, bathymetric surveys, and/or calibrated hydrology models that are simply unavailable for most of the planet (11–18). To remove this dependence on ground-based information, we show that useful estimates of absolute river discharge (i.e., in units of cubic meters per second) may be derived solely from multiple satellite images of a river, with no ground-based or a priori information whatsoever, through use of a characteristic scaling law, here termed a river's at-many-stations hydraulic geometry (AMHG). As will be shown in this paper, AMHG effectively halves the number of parameters required by traditional hydraulic geometry, thus paving the way for remote estimation of a single remaining parameter—and thus river discharge—through repeated satellite image observations along a river course. The presence of AMHG is verified in 12 of 12 rivers examined, using 88 in situ gauging stations, three field-calibrated hydrodynamic models incorporating 772 field-surveyed bathymetric cross-sections, and 42 Landsat Thematic Mapper (TM) satellite images (*SI Text*, section S1, *Materials and Methods* and Tables S1 and S2). Following a description of width AMHG, an innovative satellite discharge estimation approach is demonstrated for three major rivers, the Athabasca (Canada), Mississippi (United States), and Yangtze (China), based solely on repeated Landsat TM satellite measurements of varying instantaneous river flow widths over geographic space and time.

A Rare Advance in Hydraulic Geometry Theory

The field of hydraulic geometry was first introduced by Luna B. Leopold and Thomas Maddock, Jr., over 60 y ago (19) and continues to engage researchers in water resources, geomorphology, fisheries, aquatic ecology, and related fields today. It describes functional power-law relationships that relate river flow width (w), mean depth (d), and mean velocity (v) to discharge (Q) in accordance with the now-classic three equations:

$$w = aQ^b, \quad [1]$$

$$d = cQ^f, \quad [2]$$

$$v = kQ^m, \quad [3]$$

where $a \cdot c \cdot k$ and $b + f + m$ are theoretically constrained to unity because $Q = wdv$. In practice, the coefficients a, c, and k, and exponents b, f, and m are derived empirically through repeated field measurements at a single river cross-section (called at-a-station hydraulic geometry or AHG), or for some fixed frequency of discharge between cross-sections either downstream or on other rivers (called downstream hydraulic geometry or DHG). The depth AHG (Eq. **2**) has enormous practical utility, with empirical determinations of c and f comprising the traditional calibrated rating-curve method used by the US Geological Survey (USGS) and other water-monitoring agencies for computing

Significance

Political and practical realities limit our knowledge of water resources in many parts of the world. Here, we present a radically different approach for quantitative remote sensing of river discharge (flow rate) that is enabled by advancing a classic theory of river hydraulics and adapting it for use with satellite or aerial images. Because no ground-based information is required, the approach holds promise for addressing pressing societal, ecological, and scientific problems through global mapping of river flow.

Author contributions: L.C.S. conceived the problem and revisit of at-a-station hydraulic geometry; C.J.G. discovered at-many-stations hydraulic geometry, devised the discharge estimation method, and performed analyses; and C.J.G. and L.C.S. shared equally in research design and authorship of the paper.

The authors declare no conflict of interest.

This article is a PNAS Direct Submission. J.S.F. is a guest editor invited by the Editorial Board.

Freely available online through the PNAS open access option.

[1]To whom correspondence should be addressed. E-mail: cjgleaso@ucla.edu.

This article contains supporting information online at www.pnas.org/lookup/suppl/doi:10.1073/pnas.1317606111/-/DCSupplemental.

discharge as a function of continuously recorded water depths. Throughout six decades of research, the *b*, *f*, and *m* exponents have received abundant study, particularly in the context of elucidating theoretical and physiographic controls on their values (e.g., refs. 20–22). Eventually, they were recognized as reflective of mainly the bathymetric shape of a river channel's cross-section and argued to be unpredictably variable and site-specific (23). The *a*, *c*, and *k* coefficients, however, remain widely regarded as artifacts of the best-fit process to generate AHG. Strikingly little attention has been paid to them despite attention called to this gap by prominent authors (23–25).

This paper advances scientific understanding of hydraulic geometry by identifying a previously unnoticed correlative relationship between a river's AHG *a*, *c*, and *k* coefficients and their corresponding *b*, *f*, and *m* exponents. The correlations are readily revealed by plotting *a*–*b*, *c*–*f*, and/or *k*–*m* AHG pairs for many spatially distributed locations along a river, for example, from thousands of in situ measurements of river flow width, depth, and velocity collected between January 1, 2004, and April 9, 2013, at 88

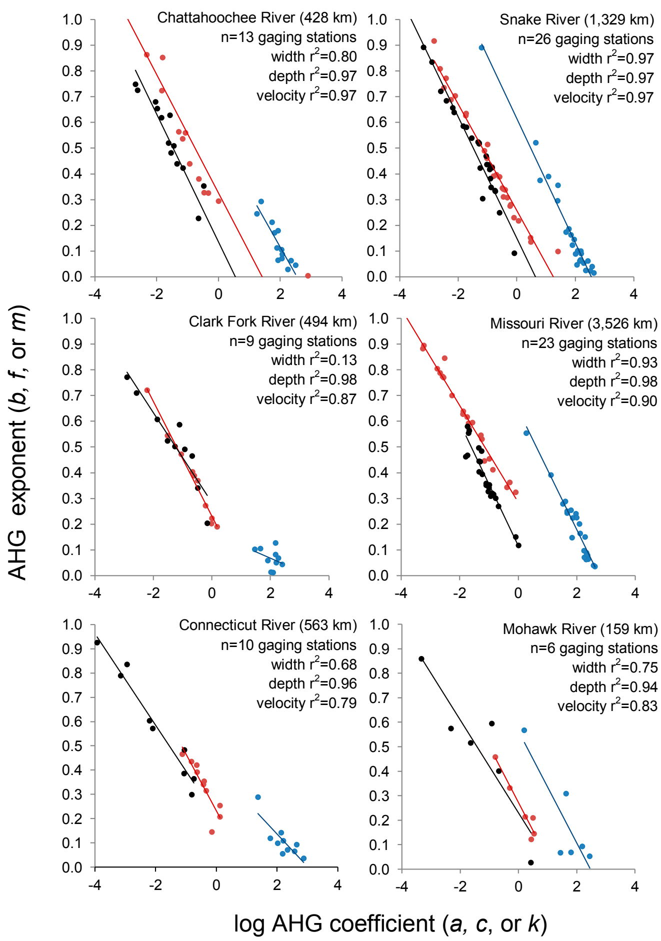

Fig. 1. AMHG derived from USGS field data. At-a-station hydraulic geometry (AHG) *a*, *c*, and *k* coefficients interact predictably with their corresponding *b*, *f*, and *m* exponents over long distances of a river, as revealed here from thousands of in situ measurements of flow width, depth, and velocity collected at 88 USGS gauging stations along six US rivers over the period 2004–2013. The discovery of these strong log-linear trends (blue, red, and black lines), here called at-many-stations hydraulic geometry or AMHG, effectively halves the traditional number of parameter(s) needed to compute river AHG and/or discharge, thus paving the way for satellite-based estimation of absolute river flow. Blue, width AMHG (*a* vs. *b*); red, depth AMHG (*c* vs. *f*); black, velocity AMHG (*k* vs. *m*).

USGS gauging station cross-sections along six prominent rivers in the United States (Fig. 1). Because these correlations are obtained simply by aggregating local AHG parameter pairs from many distributed locations along a river, they are here termed "at-many-stations hydraulic geometry," or AMHG. Although somewhat reminiscent of DHG (in that it considers longitudinal trends), AMHG differs markedly from DHG because all discharge variations are considered (not a single, bankfull discharge), the correlations are log-linear (not log-log), and the trends reflected do not follow a downstream direction. Further support for this purely empirical observation is given through consideration of limits of Eqs. **1–3** (*SI Text*, section S2 and Fig. S1).

Very significantly, the strong goodness-of fit for the observed AMHG relationships (i.e., r^2 = 0.94–0.98 for depth, r^2 = 0.13–0.97 for width, and r^2 = 0.79–0.97 for velocity; Fig. 1) indicates that, in contrast to prevailing thought (23), AHG coefficients and exponents are not unpredictable, but instead interact stably and predictably along long reaches of a river. This finding of robust depth, width, and velocity AMHG relationships essentially collapses the number of unknown AHG parameters in the three classical hydraulic geometry equations from six to three. If only one of a river's AMHG relationships is considered (as is commonly done in AHG, i.e., the traditional depth-discharge rating curve), then the number of unknown parameters is collapsed from two to one. For the purpose of river discharge estimation, this leads to the rather stunning conclusion that only one of the two traditional calibration parameters may suffice if a river's AMHG is well constrained. Although in principle any of a river's three AMHG relationships may be used for this purpose, we herewith focus on the *a*–*b* (width) AMHG, because unlike river depth or velocity, river width is straightforward to measure in satellite imagery.

Six other *a*–*b* relationships, plotted from output of field-calibrated Hydrologic Engineering Center–River Analysis System (HEC-RAS) hydrodynamic model simulations (Mississippi, Rio Grande, and Sacramento Rivers; *SI Text*, section S1) and/or simultaneous Landsat TM/gauging station observations (Mississippi, Athabasca, and Yangtze Rivers; *SI Text*, section S1) display similar behavior (r^2 = 0.60–0.99), further verifying the existence of this AMHG phenomenon (Fig. 2). Two of these datasets overlap a common area of the Mississippi River and yield virtually identical width-based AMHG, regardless of whether it is computed from a field-surveyed HEC-RAS hydrodynamic model or from Landsat TM images merged with gauging station measurements (Fig. 2, middle row, and Fig. S2). The derivation of a duplicate result from such different and independent datasets lends further support to the conclusion that AMHG scaling laws are a robust and valid characteristic of natural river behavior.

How Knowledge of a River's Width AMHG May Be Used to Estimate Discharge from Remotely Sensed Images

Based on this finding of a previously overlooked log-linear relationship between *a* and *b* (Figs. 1 and 2, and Fig. S2), the width AMHG for some user-defined length of river is appropriately defined as follows:

$$F = a_{x1,x2,\ldots xn} E^{b_{x1,x2,\ldots xn}}, \qquad [4]$$

where the subscripts $x1, x2, \ldots xn$ correspond to spatially indexed cross-section locations (up to *n* total cross-sections along the river), *a* and *b* are the classic, site-specific AHG parameters at each cross-section, and *F* and *E* are river-specific constants defining the intercept and slope, respectively, of the empirical log-linear AMHG relationship calculated from all AHG *a*–*b* pairs. Knowledge of *E* gives the intercept as well as the slope of the AMHG relationship (as *F* may be approximated from measurement of cross-sectional widths along a river; *SI Text*, section S3

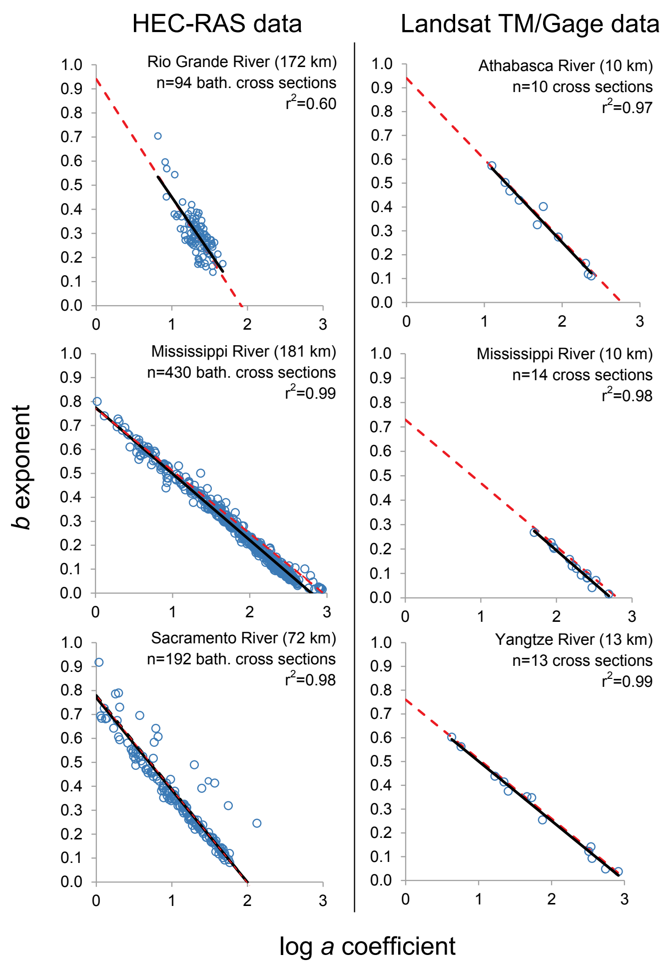

Fig. 2. AMHG derived from hydrodynamic modeling and from Landsat TM data. In situ width AMHG relationships (black lines) as derived from (*i*) simulations from three field-calibrated HEC-RAS hydrodynamic models for the Rio Grande, Mississippi, and Sacramento Rivers (United States) (left column); and (*ii*) instantaneous measurements of river surface width and discharge from Landsat Thematic Mapper (TM) satellite images over gauging stations at Fort McMurray, Alberta (Canada), Thebes, IL (United States), and Shashi, Hubei (China) (right column). The red dashed lines shows the width AMHG as approximated solely from measurements of surface width, with no knowledge of discharge or any other in situ information. The strong congruity between in situ and remotely estimated width AMHG forms the basis of quantitative remote sensing of river discharge from space.

and Table S3), thus allowing classical AHG a and b values everywhere along a sampled river length to be bridged using this single parameter E. Further mathematical discussion of AMHG and its relation to classic AHG parameters is provided in *SI Text* (section S3).

Critically, the width AMHG parameter E may be estimated from remotely sensed observations of river surface width accumulated over space and time (*SI Text*, sections S4 and S5 and Table S4), yielding remarkably accurate approximations of the river's width AMHG relationship compared with full in situ knowledge (red dashed lines, Fig. 2 and Fig. S2). From there, at least two approaches are available for computing absolute values (in cubic meters per second) of river discharge solely from satellite images: numerical optimization of AHG (as is recommended here; *SI Text*, section S7 and Fig. S3) or random seeding of plausible AHG values (*SI Text*, section S8 and Fig. S4). We here estimate local AHG from AMHG through heuristic optimization using a genetic algorithm (GA), a method that is both easily understood and parsimonious (26, 27). We adapted a previously developed GA (28) to minimize the difference in discharge calculated from AHG between pairs of cross-sections contained within ∼10-km mass-conserved river reaches (i.e., without tributaries or outflows; *SI Text*, section S7), then reach-averaged these discharges to arrive at final reported hydrographs for six rivers (Fig. 3 and *SI Text*, section S9). Crucially, the methodology detailed in *SI Text*, section S7, requires only multitemporal measurements of cross-sectional width as input data, and draws AHG values from a wide range of possible values (Table S5) derived from each river's AMHG. The method assumes that AHG is valid for all cross-sections within each river reach, which is problematic when applied to rivers with large tidal or other backwater-controlled flow regimes. However, this purely remotely sensed approach differs markedly from previous discharge estimation methodologies in that no knowledge or assumptions about channel hydraulics (e.g., mean cross-sectional depth, roughness coefficient, or energy slope), local topography, or climatic conditions are needed to estimate river discharge.

Feasibility Demonstrations and Implications for Global Water Resources

The described satellite river discharge estimation procedure yields surprisingly good results, both in terms of absolute flow magnitude (in cubic meters per second) and its ability to track relative flow changes over time. For discharge estimates obtained solely from repeated Landsat TM measurements of instantaneous river surface width (Fig. 3), the mean reach-averaged discharge root-mean-square error (RMSE) is 2,585 m^3/s (23%), 299 m^3/s (30%), and 3,772 m^3/s (20%)

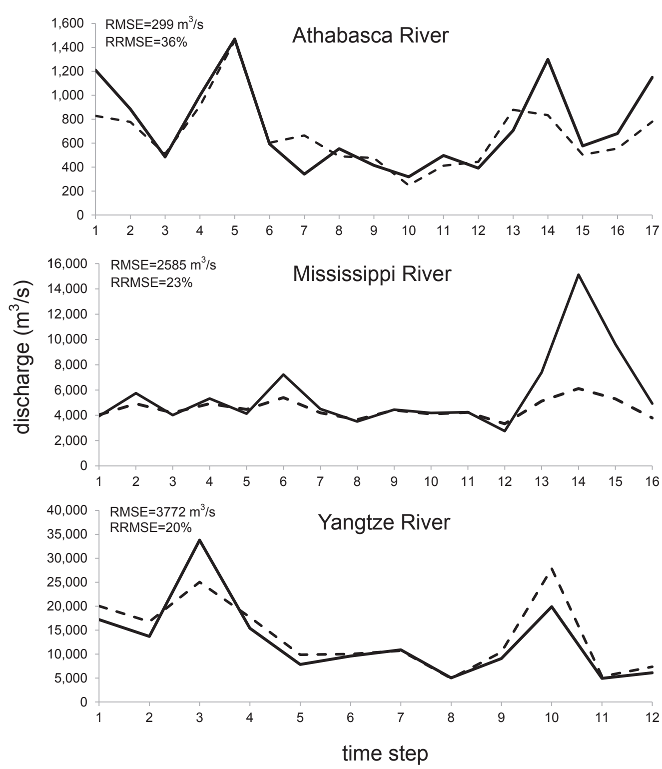

Fig. 3. Discharge estimation solely from Landsat TM images. Absolute (in cubic meters per second) river discharge hydrographs for 10- to 13-km reaches of the Athabasca, Mississippi, and Yangtze Rivers, as recorded by in situ gauging stations (solid line), and as estimated solely from Landsat TM satellite images (dashed line). The only data needed to produce the dashed-line hydrographs are repeated cross-sectional measurements of instantaneous river surface width collected over a river reach. Time step refers to chronological order of Landsat TM image acquisitions and thus varies for each river (for acquisition dates, see Table S2).

for a 10-, 10-, and 13-km reach of the Mississippi, Athabasca, and Yangtze Rivers, respectively, compared with independent discharge measurements collected at a permanent gauging stations contained within each reach (*SI Text*, section S9). These purely remotely sensed discharges also track temporal dynamics quite well (Fig. 3). The method does appear to underestimate discharges during large overbank floods (e.g., during a major June 10, 2008, event on the Mississippi River, time step 14 on Fig. 3), likely owing to breakdown of AHG power-law behavior when a river's flow overtops its banks (25).

For river discharge estimates obtained solely from repeated instantaneous surface widths output by the HEC-RAS hydrodynamic model, mean reach-averaged discharges yield similarly good results (Fig. S5), with RMSEs of 1,608 m^3/s (27%), 195 m^3/s (26%), and 29 m^3/s (1,083%) for the Mississippi, Sacramento, and Rio Grande Rivers, respectively (based on 15, 6, and 4 10-km reaches, respectively; Table S6). Like the Landsat TM results, these width-based discharge estimates also track temporal dynamics quite well (Fig. S5). Poorest performance is associated with the Rio Grande River, a semiarid, intermittently anabranching river with low flows, high geomorphic variability, and the second-weakest width AMHG seen in this study (r^2 = 0.60; Fig. 3). For further description of the sensitivities and performances of this discharge estimation method, see *SI Text*, section S9.

This paper presents an important and overlooked feature of a mature, widely used framework in water science, and uses it to advance a fundamentally different approach for estimating absolute river discharges (water fluxes) from space absent in situ measurements, calibrated hydrological models, or other a priori information. This directly mitigates a long-standing barrier of nonquantification of river flows for the vast majority of rivers on Earth, which impedes the efforts of scientists and policymakers to assess global vulnerabilities in human and ecosystem water security, compliance with transboundary river water-sharing agreements, water balance closure in climate models, flood probabilities, food chains, deforestation, and many other problems (1, 2, 29–32). Although the manually derived river width measurements described here are labor intensive, at least two methods exist for automated mapping of river widths from satellite imagery (33, 34). Merging of such automated width retrievals with the AMHG discharge estimation approach presented here would enable immediate commencement of approximate river discharge mapping for the world's large, single-thread rivers, using archived and/or forthcoming image data from aerial photographs, satellites, unmanned aerial vehicles, and any other source from which repeated images may be collected over large areas of the world's river systems.

ACKNOWLEDGMENTS. M. Durand and M. K. Mersel provided calibrated HEC-RAS model datasets, and J. Wang provided critical comments at an early stage of this research. M. Zebrowski provided graphical assistance with illustrations. Constructive, helpful reviews by two anonymous reviewers and N. D. Smith are gratefully acknowledged. This research was supported by National Aeronautics and Space Administration (NASA) Remote Sensing Theory Initiative Grant NNX12AB41G, with additional support from NASA Surface Water Ocean Topography Mission Grant NNX13AD88G, and NASA Earth and Space Sciences Fellowship NNX12AN32H.

1. Vörösmarty CJ, et al. (2010) Global threats to human water security and river biodiversity. *Nature* 467(7315):555–561.
2. Hannah DM, et al. (2011) Large-scale river flow archives: Importance, current status and future needs. *Hydrol Processes* 25:1191–1200.
3. Hunger M, Doell P (2008) Value of river discharge data for global-scale hydrological modeling. *Hydrol Earth Syst Sci* 12:841–861.
4. Stahl K, Tallaksen LM, Hannaford J, van Lanen HAJ (2012) Filling the white space on maps of European runoff trends: Estimates from a multi-model ensemble. *Hydrol Earth Syst Sci* 16:2035–2047.
5. Alsdorf DE, Lettenmaier DP (2003) Geophysics. Tracking fresh water from space. *Science* 301(5639):1491–1494.
6. Bjerklie DM, Dingman SL, Vorosmarty CJ, Bolster CH, Congalton RG (2003) Evaluating the potential for measuring river discharge from space. *J Hydrol (Amst)* 278:17–38.
7. Alsdorf DE, Rodriguez E, Lettenmaier DP (2007) Measuring surface water from space. *Rev Geophys* 45:RG2002.
8. Durand M, et al. (2010) The surface water and ocean topography mission: Observing terrestrial surface water and oceanic submesoscale eddies. *Proc IEEE* 98:766–779.
9. Syed TH, Famiglietti JS, Chambers DP (2009) GRACE-based estimates of terrestrial freshwater discharge from basin to continental scales. *J Hydrometeorol* 10:22–40.
10. Syed TH, Famiglietti JS, Chambers DP, Willis JK, Hilburn K (2010) Satellite-based global-ocean mass balance estimates of interannual variability and emerging trends in continental freshwater discharge. *Proc Natl Acad Sci USA* 107(42):17916–17921.
11. Smith LC, Isacks BL, Forster RR, Bloom AL, Preuss I (1995) Estimation of discharge from braided glacial rivers using ERS-1 SAR: First results. *Water Resour Res* 31:1325–1329.
12. Smith LC (1997) Satellite remote sensing of river inundation area, stage, and discharge: A review. *Hydrol Processes* 11:1427–1439.
13. Smith LC, Pavelsky TM (2008) Estimation of river discharge, propagation speed, and hydraulic geometry from space: Lena River, Siberia. *Water Resour Res* 44:W03427.
14. Bates PD, Horritt MS, Smith CN, Mason D (1997) Integrating remote sensing observations of flood hydrology and hydraulic modelling. *Hydrol Processes* 11:1777–1795.
15. Getirana ACV, et al. (2009) Hydrological monitoring of poorly gauged basins based on rainfall-runoff modeling and spatial altimetry. *J Hydrol (Amst)* 379:205–219.
16. Biancamaria S, et al. (2011) Assimilation of virtual wide swath altimetry to improve Arctic river modeling. *Remote Sens Environ* 115:373–381.
17. Durand M, Rodriguez E, Alsdorf DE, Trigg M (2010) Estimating river depth from remote sensing swath interferometry measurements of river height, slope, and width. *IEEE J-STARS* 3:20–31.
18. Brakenridge GR, et al. (2012) Calibration of satellite measurements of river discharge using a global hydrology model. *J Hydrol (Amst)* 475:123–136.
19. Leopold LB, Maddock T (1953) *The Hydraulic Geometry of Stream Channels and Some Physiographic Implications*, USGS Professional Paper (US Government Printing Office, Washington, DC), Vol 252.
20. Knighton AD (1975) Variations in at-a-station hydraulic geometry. *Am J Sci* 275: 186–218.
21. Park CC (1977) World-wide variation in hydraulic geometry exponents of stream channels—analysis and some observations. *J Hydrol (Amst)* 33:133–146.
22. Parker G, Wilcock PR, Paola C, Dietrich WE, Pitlik J (2007) Physical basis for quasi-universal relations describing bankfull hydraulic geometry of single-thread gravel bed rivers. *J Geophys Res* 112:F04005.
23. Phillips JD (1990) The instability of hydraulic geometry. *Water Resour Res* 26:739–744.
24. Ferguson RI (1986) Hydraulics and hydraulic geometry. *Prog Phys Geogr* 10:1–31.
25. Dingman SL (2007) Analytical derivation of at-a-station hydraulic-geometry relations. *J Hydrol (Amst)* 334:17–27.
26. Grefenstette JJ (1986) Optimization of control parameters for genetic algorithms. *IEEE Trans Syst Man Cybern* 16:122–128.
27. Deb K, Pratap A, Agarwal S, Meyarivan T (2002) A fast and elitist multiobjective genetic algorithm: NSGA-II. *IEEE Trans Evol Comput* 6:182–197.
28. Gleason CJ, Im J (2012) A fusion approach for tree crown delineation from lidar data. *Photogramm Eng Remote Sensing* 78:679–692.
29. Trenberth KE, Fasullo JT (2013) North American water and energy cycles. *Geophys Res Lett* 40:365–369.
30. Forsythe FN, Fowler HJ, Kilsby CG, Archer DR (2012) Opportunities from remote sensing for supporting water resources management in village/valley scale catchments in the upper Indus basin. *Water Resour Manage* 26:845–871.
31. Sabo JL, Finlay JC, Kennedy T, Post DM (2010) The role of discharge variation in scaling of drainage area and food chain length in rivers. *Science* 330(6006):965–967.
32. Davidson EA, et al. (2012) The Amazon basin in transition. *Nature* 481(7381):321–328.
33. Pavelsky TM, Smith LC (2008) RivWidth: A software tool for the calculation of river widths from remotely sensed imagery. *IEEE Geosci Remote Sens Lett* 5:70–73.
34. Fisher GB, Bookhagen B, Amos CB (2013) Channel planform geometry and slopes from freely available high-spatial resolution imagery and DEM fusion: Implications for channel width scalings, erosion proxies, and fluvial signatures in tectonically active landscapes. *Geomorphology* 194:46–56.